J. Fluid Mech. (1995), *vol.* 282, *pp.* 163–186

The stabilizing effect of compressibility in turbulent shear flow

By S. SARKAR

Department of Applied Mechanics and Engineering Sciences, University of California at San Diego, La Jolla, CA 92093, USA

(Received 4 March 1994 and in revised form 14 July 1994)

Direct numerical simulation of turbulent homogeneous shear flow is performed in order to clarify compressibility effects on the turbulence growth in the flow. The two Mach numbers relevant to homogeneous shear flow are the turbulent Mach number M_t and the gradient Mach number M_g. Two series of simulations are performed where the initial values of M_g and M_t are increased separately. The growth rate of turbulent kinetic energy is observed to decrease in both series of simulations. This 'stabilizing' effect of compressibility on the turbulent energy growth rate is observed to be substantially larger in the DNS series where the initial value of M_g is changed. A systematic comparison of the different DNS cases shows that the compressibility effect of reduced turbulent energy growth rate is primarily due to the reduced level of turbulence production and not due to explicit dilatational effects. The reduced turbulence production is not a mean density effect since the mean density remains constant in compressible homogeneous shear flow. The stabilizing effect of compressibility on the turbulence growth is observed to increase with the gradient Mach number M_g in the homogeneous shear flow DNS. Estimates of M_g for the mixing layer and the boundary layer are obtained. These estimates show that the parameter M_g becomes much larger in the high-speed mixing layer relative to the high-speed boundary layer even though the mean flow Mach numbers are the same in the two flows. Therefore, the inhibition of turbulent energy production and consequent 'stabilizing' effect of compressibility on the turbulence (over and above that due to any mean density variation) is expected to be larger in the mixing layer relative to the boundary layer, in agreement with experimental observations.

1. Introduction

The inhibited growth of the shear layer thickness and the turbulent stresses in the high-speed mixing layer is a well-known phenomenon (Bradshaw 1977; Kline, Cantwell & Lilley 1982; Papamoschou & Roshko 1988). For example, the thickness of a plane mixing layer at convective Mach number $M_c = 1.5$ grows at a rate which is only a third of the nominal incompressible value. However, the reasons for the strong 'stabilizing' effect of compressibility in the turbulent mixing layer remain unclear. One explanation (Sandham & Reynolds 1991; Morris, Giridharan & Lilley 1990) draws an analogy with the result of linear analysis that the growth rate of small disturbances decreases when the convective Mach number M_c increases. Here, the convective Mach number M_c is the ratio of the mean velocity difference $(U_1 - U_2)$ across the mixing layer to the sum $(c_1 + c_2)$ of the sound speeds in the two streams. Linear stability analyses (Ragab & Wu 1989; Jackson & Grosch 1990; Sandham & Reynolds 1991) show that the growth rate of the most amplified disturbance decreases as a function of M_c.

Jackson & Grosch (1990) have shown that the linear analysis results for the maximal growth rate for a wide range of values for the free-stream temperature and density fall on essentially a single curve which is a function of M_c. The similarity between the variation of disturbance growth rate as a function of M_c and the variation of the experimentally observed growth rate of shear layer thickness as a function of M_c has prompted the argument that linear stability analysis explains the compressibility effect of reduced mixing. However, it is unclear how and why simple linear theory applies to the fully turbulent mixing layer.

Another explanation of the reduced mixing of the high-speed mixing layer has been advanced by Zeman (1990) and Sarkar *et al.* (1991*b*), who suggest that the dissipative effect of dilatational velocity fluctuations (such fluctuations have $\nabla \cdot \boldsymbol{u} \neq 0$) becomes progressively more important when the turbulent Mach number M_t increases, reduces the turbulent energy, and thereby decreases turbulent mixing. The turbulent Mach number M_t is the ratio of the r.m.s. (root mean square) velocity fluctuation u to the speed of sound c. Turbulence models developed by Zeman (1990) and Sarkar *et al.* (1991*b*) which parametrize the dilatational correlations as functions of M_t have been able to capture the decreased growth rate of the high-speed mixing layer. However, the hypothesis that dilatational effects lead to the stabilizing effect of compressibility needs direct validation.

Compressibility effects in the high-speed boundary layer are different from those in the high-speed mixing layer. When the free-stream Mach number M_∞ of the boundary layer increases, there is a moderate decrease in skin friction and thickness growth rate which is directly due to the reduction of density from its free-stream value and the consequent reduction in momentum transport by the Reynolds shear stress. In the case of the compressible mixing layer, an increase in the convective Mach number M_c leads to a dramatic reduction in the growth rate of the shear layer thickness, a reduction which is far larger than can be explained by the density variation. The discrepancy between compressibility effects in free shear layers and wall boundary layers is not understood. A theoretical explanation for the reduced growth rate of the high-speed mixing layer should account for this crucial difference between turbulent free shear flows and wall-bounded flows in the high-speed regime.

Owing to the limitations of current computer hardware, three-dimensional direct numerical simulations (DNS) of the compressible mixing layer or the compressible boundary layer have not been performed at Reynolds number sufficiently high for the turbulence to be fully developed. It is relatively easier to simulate homogeneous turbulent flows at realistic turbulence Reynolds numbers, and then perform a parametric DNS study that compares results from a few different cases. In the present paper, simulations of homogeneous shear flow, a flow with constant mean shear rate, are described. Homogeneous shear flow retains the feature of sustenance of turbulent kinetic energy by mean shear common to a variety of turbulent shear flows. Compressible homogeneous shear flow has been studied previously with DNS by Feiereisen *et al.* (1982), and more recently by Sarkar, Erlebacher & Hussaini (1991*a*), and Blaisdell, Mansour & Reynolds (1993). Although the two later DNS investigations did find that increased levels of compressibility lead to decreased levels of turbulence just as observed in experiments on the high-speed mixing layer, a systematic comparison of different cases to identify possible causes for this 'stabilizing' effect of compressibility was not performed. Furthermore, the studies neglected to discriminate between the gradient Mach number M_g and the turbulent Mach number M_t. The gradient Mach number is $M_g = Sl/c$, where $S = \mathrm{d}\bar{U}/\mathrm{d}y$ is the mean shear rate, l a representative integral lengthscale of the turbulence in the direction of shear, and c the

speed of sound. The parameter M_g can be viewed as the ratio of an acoustic time l/c for a large eddy to the mean flow timescale $1/S$. Durbin & Zeman (1992), in their RDT (rapid distortion theory) analysis of homogeneous compressed turbulence, recognized that a parameter similar to the gradient Mach number that is defined by $\Delta m = Dl/c$ with $D = |\nabla \cdot U|$ is one of the relevant parameters; however, these authors considered only the limit $\Delta m \ll 1$. Later, Jacquin, Cambon & Blin (1993), and Cambon, Coleman & Mansour (1993), showed, again for homogeneous compressed turbulence with large mean compression rate, that compressible RDT results are sensitive to Δm. It should be noted that the RDT restriction of high mean distortion rate relative to the large-scale turbulence distortion rate does not apply to the present simulations.

Since the gradient Mach number M_g introduced in the present work is based on the mean velocity field, like the convective Mach number M_c, it is important to compare and contrast these two Mach numbers. There is of course a similarity, because $M_g = Sl/c$ can be viewed as a ratio of the mean velocity difference Sl across a 'large-scale eddy' to the speed of sound, just as M_c is related to the ratio of the mean velocity difference across the two streams in a mixing layer to the speed of sound. However, there are essential differences. The parameter M_g is a field quantity which varies across an inhomogeneous shear layer, unlike M_c. Moreover, M_g differs among shear flows such as the mixing layer, boundary layer and the wall jet since the variation of mean velocity field and turbulence lengthscale is different in these flows even if the overall velocity difference across the flows is the same. In fact, we will show later in this paper that the value of M_g is much larger for the supersonic mixing layer than the supersonic boundary layer even if the mean flow Mach number has the same value in the two flows.

In our earlier DNS studies (Sarkar *et al.* 1991 *a*) of compressible homogeneous shear flow, the speed of sound was varied keeping all other parameters fixed which led to the simultaneous change of initial gradient Mach number M_{g0} and initial turbulent Mach number M_{t0}. Similarly, M_{g0} and M_{t0} were simultaneously increased (or decreased) in the independent DNS investigation of Blaisdell *et al.* (1993). The present study performs two series of new simulations that comprise six different cases to address the following questions: (i) How do the gradient Mach number and turbulent Mach number *individually* effect the flow evolution? and (ii) What are the probable reasons for any compressibility effects on the flow evolution due to the variation of these Mach numbers? In series A of the simulations, M_{g0} is varied keeping M_{t0} constant and vice versa in series B. It should be noted that M_g and M_t are different parameters because their ratio $M_g/M_t = Sl/u$ is not a constant, that is, Sl/u can depend on other factors such as the flow geometry, compressibility, wall effects and initial/boundary conditions. Thus, among incompressible flows, the log region in the boundary layer, equilibrium homogeneous shear flow, and the near-wall region in the boundary layer have progressively larger values of Sl/u and correspondingly different turbulence structure and growth rates. For example, Lee, Kim & Moin (1990) have shown that incompressible homogeneous shear flow with initial Sl/u that is sufficiently larger than the equilibrium value exhibits low- and high-speed streaks just as in near-wall turbulence.

2. Preliminary analysis

The compressible Navier–Stokes equations provide the mathematical model for the problem. After performing the Reynolds decomposition into mean and fluctuating parts of the velocity, a system of equations can be obtained for the evolution of the

instantaneous density ρ^*, velocity fluctuation $u_i^{*\prime}$, and the instantaneous pressure p^*. The superscript $*$ is used to denote a dimensional variable, the overbar is used to denote an averaged variable, and the prime is used to denote fluctuations in a variable with respect to its average. A tilde will be used later for denoting mass-weighted or Favre average. The following equations are a specialization of the general equations to the homogeneous shear flow problem where the mean velocity is $\bar{U}_1^* = Sx_2^*$, and S is a constant:

$$\partial_t \rho^* + \bar{U}_i^* \rho^*_{,i} + (\rho^* u_i^{*\prime})_{,i} = 0, \tag{1}$$

$$\partial_t(\rho^* u_i^{*\prime}) + \bar{U}_j^*(\rho^* u_i^{*\prime})_{,j} + (\rho^* u_j^{*\prime} u_i^{*\prime})_{,j} = -p^*_{,i} - S\rho^* u_2^{*\prime}\delta_{i1} + \tau^{*\prime}_{ij,j}, \tag{2}$$

$$\partial_t p^* + \bar{U}_j^* p^*_{,j} + (u_j^{*\prime} p^*)_{,j} = -(\gamma-1) p^* u^{*\prime}_{j,j} + (\gamma-1)\kappa T^*_{,jj} + (\gamma-1)\Phi^*, \tag{3}$$

$$p^* = \rho^* R T^*, \tag{4}$$

where $\Phi^* = \tau^{\prime *}_{ij} u^{*\prime}_{i,j} + \mu S^2$ is the dissipation function, μ the molecular viscosity, R the gas constant, γ the ratio of specific heats, and κ the thermal conductivity. The fluid properties μ, R and κ are taken to be constant to simplify the problem. The fluctuating viscous stress is

$$\tau^{\prime *}_{ij} = \mu(u^{*\prime}_{i,j} + u^{*\prime}_{j,i}) - \tfrac{2}{3}\mu u^{*\prime}_{k,k}\delta_{ij}. \tag{5}$$

We wish to determine the variables that parametrize compressibility effects on the turbulence evolution. One method is to determine the conditions under which the acoustic timescale l_0/c_0 becomes important for the behaviour of a given turbulence velocity fluctuation u_0 with lengthscale l_0. For this purpose, we non-dimensionalize (1)–(4) with l_0/c_0 as the timescale, the initial mean density ρ_0 as the density scale, the initial mean temperature T_0 as the temperature scale, u_0 the fluctuating velocity scale, U_0 the mean velocity scale, and l_0 the lengthscale. The instantaneous pressure is non-dimensionalized by $\rho_0 u_0^2$. The exception is the first term on the right-hand side of (3) which is explicitly split into a mean pressure and fluctuating pressure, and the mean pressure is non-dimensionalized by the initial mean pressure P_0 so that $\bar{P} = \bar{P}^*/P_0 = O(1)$. The non-dimensionalization adopted here uses a hybrid scaling because incompressible scaling $\rho_0 u_0^2$ is used for pressure variation while acoustic scaling l/c_0 is used for the time variation.

The non-dimensional equations become

$$\partial_t \rho + M_0 \bar{U}_i \rho_{,i} + M_{t0}(\rho u_i')_{,i} = 0, \tag{6}$$

$$\partial_t(\rho u_i') + M_0 \bar{U}_j(\rho u_i')_{,j} + M_{t0}(\rho u_j' u_i')_{,j} = -M_{t0} p'_{,i} - M_{g0}\rho u_2' \delta_{i1} + \frac{M_{t0}}{Re_0}\tau'_{ij,j}, \tag{7}$$

$$\partial_t p + M_0 \bar{U}_j p_{,j} + M_{t0}(u_j' p)_{,j} = -\frac{(\gamma-1)}{\gamma M_{t0}}\bar{P} u'_{j,j} - (\gamma-1) M_{t0} p' u'_{j,j} + \frac{\gamma M_{t0}}{Pr_0 Re_0}(p/\rho)_{,jj} + \frac{(\gamma-1) M_{t0}}{Re_0}\Phi, \tag{8}$$

$$T = \frac{\gamma M_{t0}^2 p}{\rho}. \tag{9}$$

The non-dimensional parameters unrelated to the speed of sound that appears in (6)–(9) are the Reynolds numbers $Re_0 = u_0 l_0/\nu_0$ and the Prandtl number $Pr_0 = \mu C_p/\kappa$. Since the mean convection term that contains $\bar{U}_i$ can be removed in the special case of homogeneous turbulence by transforming the equations to a frame moving with the mean velocity, the mean Mach number M_0 does not affect the evolution of the flow

variables in that moving reference frame. Thus, the only two 'compressibility' parameters in the equations for homogeneous shear flow are the *turbulent Mach number* $M_{t0} = u_0/c_0$ and the *gradient Mach number* $M_{g0} = Sl_0/c_0$. For a general flow, the gradient Mach number can be defined by $M_{g0} = Sl_0/c_0$ where $S = (\bar{U}_{i,j}\,\bar{U}_{i,j})^{1/2}$ and l_0 an appropriate integral lengthscale. In the case of shear flow, l_0 is chosen to be the integral lengthscale of the streamwise fluctuating velocity in the shearing direction x_2.

Equation (7) suggests that the fluid momentum may change significantly on the acoustic timescale if $M_{t0} = O(1)$ or $M_{g0} = O(1)$. Similarly, (6) and (8) show that if $M_{t0} = O(1)$ the variation of fluid density and pressure on the acoustic timescale can be significant. Thus, it is clear that compressibility effects on the flow evolution increase when either M_{g0} or M_{t0} increases. In the present DNS study, the quantities M_{g0} and M_{t0} are considered to be the compressibility parameters and varied among different cases.

We note that the above discussion of compressibility effects on the flow evolution is relevant only after any initial transients in the flow have subsided. The role of initial conditions in the evolution of compressible isotropic turbulence has been previously investigated by Erlebacher *et al.* (1990) with a DNS of the full system and with a low-M_{t0} asymptotic analysis where the nonlinear and viscous terms were dropped. The reduced equations in the analysis constitute a hyperbolic system whose eigenvalues show strong asymmetry essentially due to the $1/M_{t0}$ scaling of the right-hand side of (8) versus the M_{t0} scaling of the right-hand side of (7). We found that, owing to the asymmetry in the eigenvalues, dilatational velocity fluctuations or pressure fluctuations can grow rapidly on the acoustic timescale from their respective initial values under some circumstances, and furthermore classified the conditions which lead to the initial transients. The initial conditions in this study have been chosen so as to remove the influence of such initial transients.

The turbulent kinetic energy $K = \frac{1}{2}\widetilde{u_i'' u_i''}$, where the Favre average $\widetilde{u_i'' u_i''} = \overline{\rho u_i'' u_i''}/\bar{\rho}$, is an estimate of the energy associated with the velocity fluctuations. For the homogeneous turbulence considered here, K is computed as a volume average over the computational domain. The turbulent kinetic energy is a function of time and the non-dimensional parameter $\Lambda(t) = (1/SK)(\mathrm{d}K/\mathrm{d}t)$ describes the instantaneous value of its temporal growth rate. It may be expected that physical effects that decrease Λ in homogeneous shear flow will inhibit turbulent energy levels and thereby inhibit shear layer growth in inhomogeneous turbulent shear flows as well. In fact, it is shown below through an analogy that the coefficient C_δ in the following commonly accepted expression for the streamwise growth rate of a mixing layer between two streams with uniform speeds U_1 and U_2,

$$\frac{\mathrm{d}\delta}{\mathrm{d}x} = C_\delta \frac{U_1 - U_2}{U_1 + U_2} \tag{10}$$

is proportional to Λ.

Consider a self-similar, plane mixing layer between two streams of velocity U_1 and U_2. The kinetic energy K in such a mixing layer is given by

$$K = C_0(U_1 - U_2)^2 f(\eta), \tag{11}$$

where C_0 is a constant, the similarity variable $\eta = y/\delta(x)$, and $\delta(x)$ is the shear layer thickness. Let K^* be the kinetic energy integrated across the transverse direction, that is

$$K^* = \int_{-\infty}^{+\infty} K\,\mathrm{d}y = C_0(U_1 - U_2)^2 \delta \int_{-\infty}^{+\infty} f(\eta)\,\mathrm{d}\eta. \tag{12}$$

From (12), it can be shown that

$$\frac{1}{K^*}\frac{\mathrm{d}K^*}{\mathrm{d}x} = \frac{1}{\delta}\frac{\mathrm{d}\delta}{\mathrm{d}x}. \tag{13}$$

We now consider homogeneous shear flow, $U(y) = Sy$ with S a constant. The temporal growth rate of the turbulent kinetic energy $K(t)$ is described by the non-dimensional variable A defined by

$$A = \frac{1}{SK}\frac{\mathrm{d}K}{\mathrm{d}t}, \tag{14}$$

where S is the constant shear rate. Physical experiments (Tavoularis & Karnik 1989) and DNS (Rogers, Moin & Reynolds 1987) support the notion that in the case of incompressible homogeneous shear flow, the turbulence eventually grows exponentially, that is $A(t) \to A_\infty$ (a constant) for large t. Although this picture of turbulence is consistent with available data, there is no rigorous proof that the turbulence grows exponentially for all time. In any case, A is a useful non-dimensional estimate of the instantaneous growth rate of K. Assume that the temporal evolution of the turbulent kinetic energy can be transformed into a spatial evolution of K^* by the transformation $x = U_c t$, where U_c is a characteristic convection velocity given by

$$U_c = C_2(U_1 + U_2), \tag{15}$$

where C_2 is a constant, and U_1 and U_2 are the velocities at the top and bottom of the shear layer, respectively. Then (14) can be transformed into a relation for the equivalent spatial growth rate

$$\frac{1}{K^*}\frac{\mathrm{d}K^*}{\mathrm{d}x} = \frac{A_\infty S}{U_c} = \frac{A_\infty(U_1 - U_2)}{\delta C_2(U_1 + U_2)}, \tag{16}$$

where A_∞ is the constant, large-time value of the kinetic energy growth rate.

Now we draw an analogy between the homogeneous shear layer and the mixing layer, and equate the right-hand side of (13) and (16) to obtain

$$\frac{\mathrm{d}\delta}{\mathrm{d}x} = \frac{A_\infty}{C_2}\frac{U_1 - U_2}{U_1 + U_2}. \tag{17}$$

According to the analogy, the growth rate of the mixing layer thickness is proportional to the asymptotic growth rate of turbulent kinetic energy in the corresponding homogeneous shear flow. Furthermore, (17) implies that a constant value of A_∞ in the homogeneous shear flow problem is consistent with the linear growth rate, $\mathrm{d}\delta/\mathrm{d}x \propto (U_1 - U_2)/(U_1 + U_2)$ (Schlichting 1979), seen in fully developed constant-density mixing layers if the coefficient C_2 in (15) for the convection velocity U_c is a constant independent of the free-stream velocities.

In summary, this section establishes that the gradient Mach number and the turbulent Mach number should be considered as important compressibility parameters in homogeneous shear flow. Furthermore, it is shown that the behaviour of the normalized temporal growth rate of the turbulent kinetic energy, $A = (1/SK)(\mathrm{d}K/\mathrm{d}t)$, as a function of the gradient and turbulent Mach numbers is important because of its connection to shear layer growth in more general turbulent shear flows.

3. DNS method

The algorithm for the DNS of compressible homogeneous shear flow is essentially identical to the spectral collocation, third-order Runge–Kutta algorithm which was used in our previous simulations. Details can be found in Sarkar *et al.* (1991*a*). All the simulations were performed on a 128^3 spatial grid in a cube of side 2π. Each simulation had the same initial data which corresponded to uniform density $\rho = 1$, solenoidal velocity fluctuations, pressure fluctuations calculated from the usual incompressible Poisson equation, and temperature obtained from the equation of state of an ideal gas. Such a choice minimizes the buildup of compressibility effects due to initial transients from incompatible initial conditions. The initial velocity is a Gaussian random field whose energy spectrum $E(k) \propto k^4 \exp(-2k^2/k_m^2)$ with $k_m = 18$. The flow evolution is governed by the following parameters which need to be prescribed: the shear rate S, the viscosity ν, the thermal diffusivity $\kappa/\rho_0 C_p$, the initial mean speed of sound c_0, the initial r.m.s. (root mean square) velocity u_0, and the initial turbulence lengthscale l_0. The corresponding non-dimensional parameters are M_{g0}, M_{t0}, $Re_{\lambda 0}$, and Pr_0 which are computed as follows: $M_{g0} = Sl_0/\bar{c}_0$, where S is the constant mean shear rate, l_0 the initial integral lengthscale of u in the transverse shearing direction and $\bar{c}_0$ the initial mean speed of sound; $M_{t0} = u_0/\bar{c}_0$, where $u_0 = (2K_0)^{1/2}$ and K_0 is the initial turbulent kinetic energy; $Re_{\lambda 0} = u_0 \lambda_0/\nu$, where the Taylor microscale is $\lambda_0 = u_0/\omega_0$, and $\omega_0 = (\omega_i \omega_i)^{1/2}$ is the r.m.s. vorticity; and $Pr_0 = \mu C_p/\kappa$.

Two series of simulations labelled A and B, respectively, were performed. In series A, the gradient Mach number M_{g0} is progressively increased in cases A1–A4 by changing the shear rate S, all other non-dimensional parameters remaining the same. In series B, the turbulent Mach number M_{t0} is progressively increased in B1 to B3, all other non-dimensional parameters remaining the same. Both S and c were appropriately changed in series B so as to vary M_{t0} while M_{g0} simultaneously remains constant. Table 1 gives the non-dimensional parameters applicable to the simulations performed here. Note that Case A1 is the same case as Case B3 so that there are a total of six different simulations.

The range of variation of M_{g0} and M_{t0} is chosen to cover a reasonable portion of parameter space with case B1 as an example with low gradient and turbulent Mach numbers, and case A4 as an example with high gradient and turbulent Mach numbers. The constant value $M_{t0} = 0.4$ in series A is chosen to be somewhat high so that $(Sl/u)_0 = M_{g0}/M_{t0}$ does not become so large as to cause the turbulence evolution to be dominated by linear effects (rapid distortion theory). The initial value $(Sl/u)_0$ varies between 0.55 and 3.3 in series A. The Prandtl number is chosen to be $Pr_0 = 0.7$ since the flow of air is considered here. The large scales of turbulence acquire energy due to the mean shear while the energy of the small scales grows due to the increase in turbulence Reynolds number and consequent increase in nonlinear energy transfer. Thus, the integral lengthscale l increases and the Kolmogorov lengthscale η decreases with time. The simulations were terminated when either η became small enough to cause insufficient resolution of the small scales by the grid, or when l became large enough for the periodic boundary conditions to affect the growth of the large scale. The termination time of the simulations varied between $St = 15$ and 20. The turbulent Reynolds number increases with time and its value at the end of the simulations varied between $Re_\lambda = 35$ and 42 which indicates that the velocity field becomes turbulent, albeit with moderate Reynolds number. Since the turbulence is spatially homogeneous, turbulence statistics and correlations at a given time are obtained by averaging over the 128^3 points in the computational domain.

	Case	M_{g0}	M_{t0}	$Re_{\lambda 0}$	Pr_0	$(SK/\epsilon)_0$
(*a*)	A1	0.22	0.40	14	0.7	1.8
	A2	0.44	0.40	14	0.7	3.6
	A3	0.66	0.40	14	0.7	5.4
	A4	1.32	0.40	14	0.7	10.8
(*b*)	B1	0.22	0.13	14	0.7	5.4
	B2	0.22	0.20	14	0.7	3.6
	B3	0.22	0.40	14	0.7	1.8

TABLE 1. Parameters for the DNS: (*a*) series A, (*b*) series B.

4. DNS results on the growth of turbulent energy

The compressibility effect on the evolution of turbulent kinetic energy $K = \frac{1}{2}\widetilde{u_i' u_i'}$ is discussed here. The non-dimensional parameter $\Lambda = (1/SK)(\mathrm{d}K/\mathrm{d}t)$ describes the temporal growth rate of the turbulent kinetic energy. It was shown in §2 that the behaviour of Λ is of fundamental interest.

The equation for turbulent kinetic energy K is now considered to identify the factors that could influence the growth rate. The equation for the evolution of K in homogeneous shear flow is

$$\mathrm{d}K/\mathrm{d}t = \mathscr{P} - \epsilon_s - \epsilon_c + \overline{p'd'}/\bar{\rho}, \tag{18}$$

where $\mathscr{P} = -S\widetilde{u_1' u_2'}$ is the production, $\epsilon_s = \bar{\nu}\overline{\omega_i' \omega_i'}$ the solenoidal dissipation rate, $\epsilon_c = \frac{4}{3}\bar{\nu}\overline{d'^2}$ the compressible dissipation rate, and $\overline{p'd'}$ the pressure–dilatation. Here ω_i' is the fluctuating vorticity, and d' is the fluctuation in dilatation ($\boldsymbol{\nabla}\cdot\boldsymbol{u}$). It is useful to work with an evolution equation for the growth rate $\Lambda = (1/SK)(\mathrm{d}K/\mathrm{d}t)$, an equation which is obtained from (18) to be

$$\begin{aligned}\Lambda &= -2b_{12} - \frac{\epsilon_s}{SK} - \frac{\epsilon_c - \overline{p'd'}/\bar{\rho}}{SK} \\ &= -2b_{12}\left(1 - \frac{\epsilon_s}{\mathscr{P}}\right) - \frac{\epsilon_c - \overline{p'd'}/\bar{\rho}}{SK},\end{aligned} \tag{19}$$

where $b_{12} = \widetilde{u_1' u_2'}/2K$ is the Reynolds shear stress anisotropy. The last term in (19) represents the explicit influence of compressibility through dilatational effects. In the incompressible case (Speziale 1991), it is generally accepted that homogeneous shear flow turbulence evolves to a state with constant values of b_{12} and $\epsilon_s/\mathscr{P}$, and therefore, from (19), Λ also approaches a constant equilibrium value Λ_∞. It is clear from (19) that a change in the equilibrium value Λ_∞ in homogeneous shear flow with increasing compressibility can be due to any of the following: (i) a change in the magnitude of b_{12} which implies a more (or less) 'efficient' production mechanism, (ii) a change in $\epsilon_s/\mathscr{P}$, the relative dissipation of the turbulence, and (iii) a change in $(\epsilon_c - \overline{p'd'}/\bar{\rho})/SK$, which represents dilatational effects.

4.1. *Results from series A*

Figure 1 shows the values of Λ at integral values of St in the simulation. It is clear that there is a systematic decrease of the asymptotic (large St) value Λ_∞ of the turbulence growth rate when M_{g0} increases in cases A1–A4. For example, case A4 with $M_{g0} = 1.32$ has $\Lambda_\infty \simeq 0.03$, which is more than a factor of 3 smaller than the corresponding value of $\Lambda_\infty \approx 0.11$ in case A1 with $M_{g0} = 0.22$.

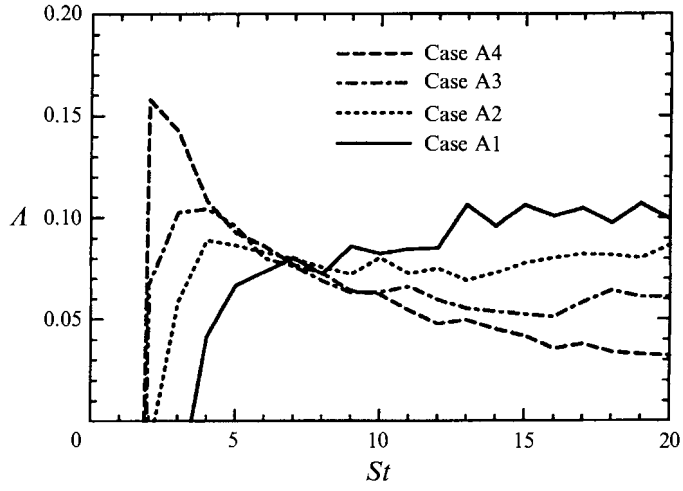

FIGURE 1. Evolution of the turbulent energy growth rate A for series A of the homogeneous shear DNS. Note that $A = (1/SK)(\mathrm{d}K/\mathrm{d}t)$, where K is the turbulent kinetic energy and S is the mean shear rate.

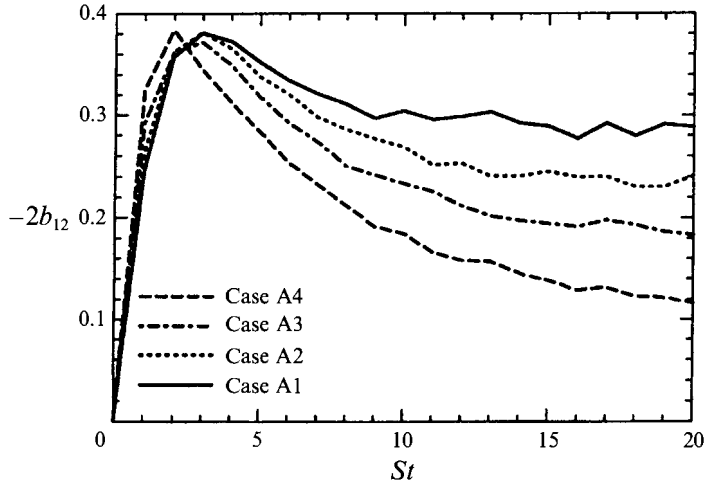

FIGURE 2. Evolution of the non-dimensional production $\mathscr{P}/SK = -2b_{12}$ in series A of the homogeneous shear DNS.

The terms on the right-hand side of (19) have been evaluated and compared in order to identify possible causes for the reduced growth rate of K. Figure 2 shows the evolution of the non-dimensional production ($\mathscr{P}/SK = -2b_{12}$). By $St = 20$, the turbulence eventually evolves to approximately constant values of Reynolds shear stress anisotropy in each case. Furthermore, the long-time values of b_{12} show a systematic decrease with the corresponding value of M_{g0}. The magnitude of $-2b_{12}$ in case A4 is smaller by a factor of 3 relative to that in case A1. Thus, the efficiency of turbulent production by the mean shear is strongly inhibited when the gradient Mach number increases.

The evolution of $\epsilon_s/\mathscr{P}$ is shown in figure 3(*a*). After an initial transient, there is only a slight difference between the different cases which is far too small to cause the large reduction in A. For example, $\epsilon_s/\mathscr{P}$ at $St = 20$ varies between 0.5 and 0.6 for cases

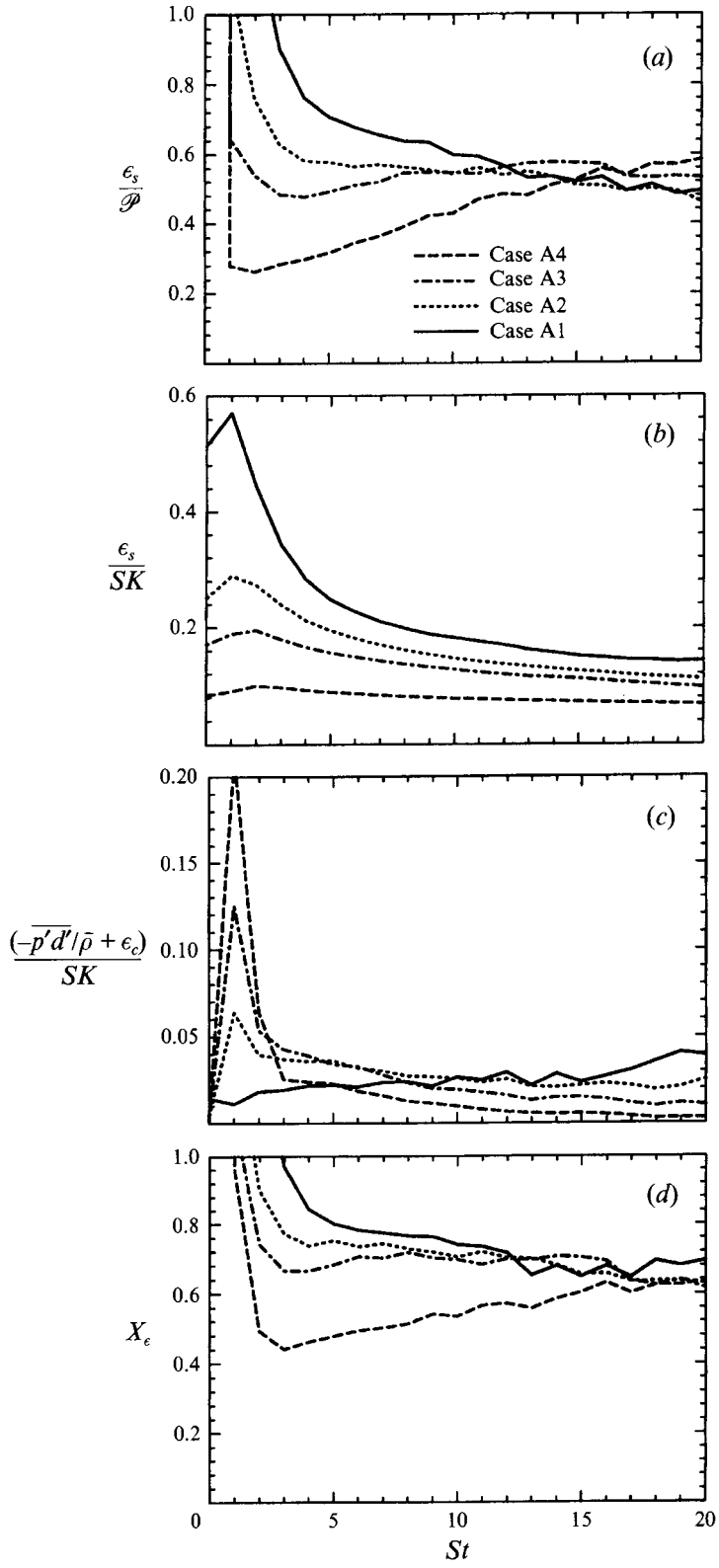

FIGURE 3(*a–d*). For caption see facing page.

A1–A4. The 20% increase in the relative dissipation $\epsilon_s/\mathscr{P}$ in case A4 relative to case A1 is a small effect compared to the factor of 3 decrease in the non-dimensional turbulent production $(-2b_{12})$. Figure 3(*b*) shows the evolution of the normalized dissipation ϵ_s/SK. The long-time values of ϵ_s/SK show a systematic decrease from case A1 to A4. Since $\epsilon_s/SK = -2(\epsilon_s/\mathscr{P})\,b_{12}$, such a decrease is consistent with compressibility decreasing the value of $-b_{12}$ (in figure 2) while having very little effect on $\epsilon_s/\mathscr{P}$ (in figure 3*a*).

Figure 3(*c*) shows the behaviour of the dilatational terms. Although small, the normalized dilatational term in figure 3(*c*) is not negligible; its value at the end of the simulation is in the range of 10–30% of the growth rate Λ of the corresponding case. Owing to a similar observation in our earlier simulations (Sarkar *et al.* 1991*a*), we attributed significant importance to dilatational terms. However, the systematic comparison of the different DNS cases conducted in the present study shows that the dilatational terms do not lead to the compressibility effect of decreased growth rate of turbulent kinetic energy. This can be seen by comparing the different curves in figure 3(*c*). The difference in the normalized dilatational terms between the various cases is small and also of the wrong sign to explain the difference in the values of Λ_∞ between these cases. For instance, the values for the dilatational term $(\epsilon_c - \overline{p'd'}/\bar{\rho})/SK$ are smaller for $St > 15$ in case A4 relative to case A1, implying that dilatational effects would increase the growth rate in case A4 relative to case A1, contrary to the observed decrease in Λ.

Equation (19) for Λ can be rewritten as

$$\Lambda = -2b_{12}(1 - X_\epsilon), \tag{20}$$

where the influence of all terms other than the production term is lumped into X_ϵ which is given by

$$X_\epsilon = \frac{\epsilon_s + \epsilon_c - \overline{p'd'}/\bar{\rho}}{\mathscr{P}}. \tag{21}$$

Figure 3(*d*) shows that, after the initial transient, X_ϵ becomes approximately constant and shows very little difference for $St > 15$ among the different cases. Thus, the large reduction in the value of Λ is almost wholly due to the large reduction in the magnitude of Reynolds shear stress anisotropy b_{12}.

For homogeneous flow, the Helmholtz decomposition gives a unique split of the velocity field into incompressible and compressible components, that is $\boldsymbol{u} = \boldsymbol{u}^I + \boldsymbol{u}^C$, where $\boldsymbol{\nabla}\cdot\boldsymbol{u}^I = 0$ and $\boldsymbol{\nabla}\times\boldsymbol{u}^C = 0$. The DNS data base is investigated to ascertain whether the dilatational component $\boldsymbol{u}^C$ is explicitly responsible for the reduced production. The Helmholtz decomposition leads to the following expression for the Reynolds shear stress anisotropy:

$$b_{12} = (1 - \chi_k)\, b_{12}^I + \chi_k\, b_{12}^C, \tag{22}$$

where $\chi_k = K^C/K$ is the compressible fraction of turbulent kinetic energy, $b_{12}^I = \widetilde{u_1^I u_2^I}/2K^I$, and $b_{12}^C = (\widetilde{u_1' u_2'} - \widetilde{u_1^I u_2^I})/2K^C$. It is found that the last term on the right-hand side of (22) is much smaller than the first term on the right-hand side primarily because $\chi_k < 10\%$ in all the simulations considered here. This implies that the reduced b_{12} of the *solenoidal velocity component* is responsible for the reduction in the overall value of b_{12} at high gradient Mach numbers.

Thus, the DNS results of series A indicate that the large reduction of the turbulence growth rate that occurs when the gradient Mach number M_{g0} increases is primarily due

FIGURE 3. Evolution of (*a*) the relative dissipation $\epsilon_s/\mathscr{P}$, (*b*) the normalized dissipation ϵ_s/SK, (*c*) the dilatational terms in the K-equation, and (*d*) X_ϵ, the ratio of the sum of dissipation and dilatational terms to the production term in the K-equation for Series A of the homogeneous shear flow DNS.

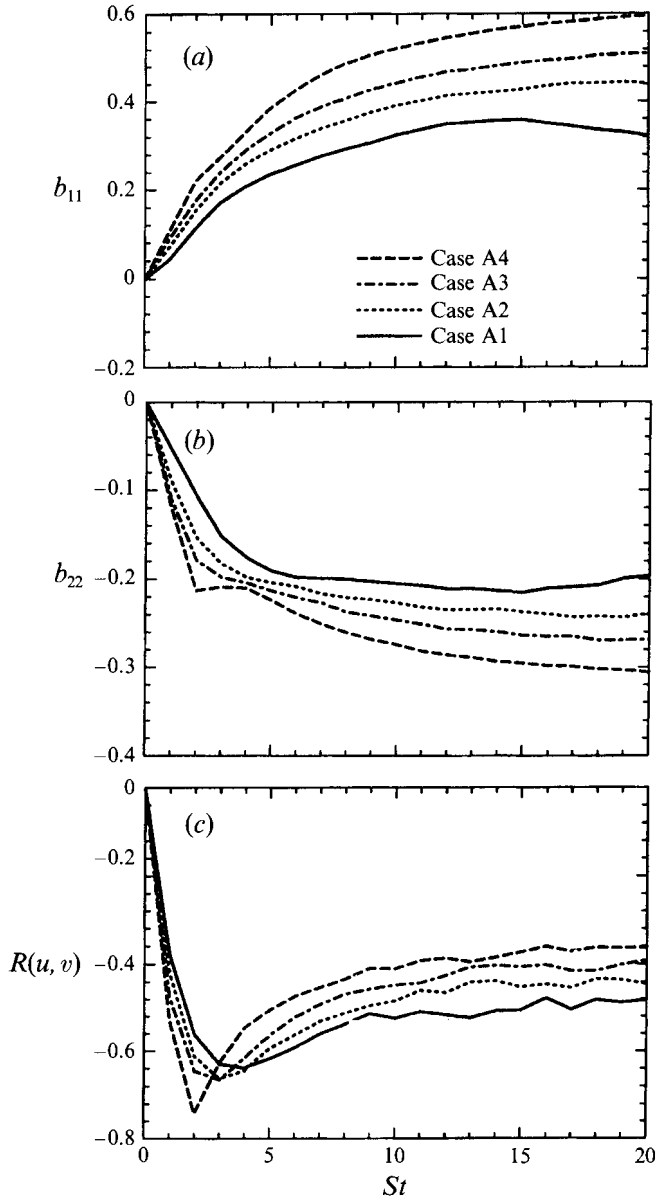

FIGURE 4. Evolution of (*a*) the streamwise, (*b*) the transverse Reynolds stress anisotropy, and (*c*) the shear stress correlation coefficient, in series A of the homogeneous shear DNS.

to the reduced Reynolds shear stress anisotropy of the solenoidal velocity component and not due to the explicit dilatational terms.

The long-time values of the Reynolds shear stress anisotropy b_{12} exhibit a systematic decrease in magnitude from cases A1 to A4 as seen in figure 2. The effect of compressibility on the other components of the Reynolds stress tensor $b_{ij} = \widetilde{u_i'' u_j''}/2K - \frac{1}{3}\delta_{ij}$ is also of interest. Figures 4(*a*) and 4(*b*) show that there is a systematic increase in the magnitude of the streamwise and transverse anisotropies, respectively, from case A1 to case A4. From these results, it can be deduced that the pressure–strain correlation tensor in homogeneous shear flow is significantly changed

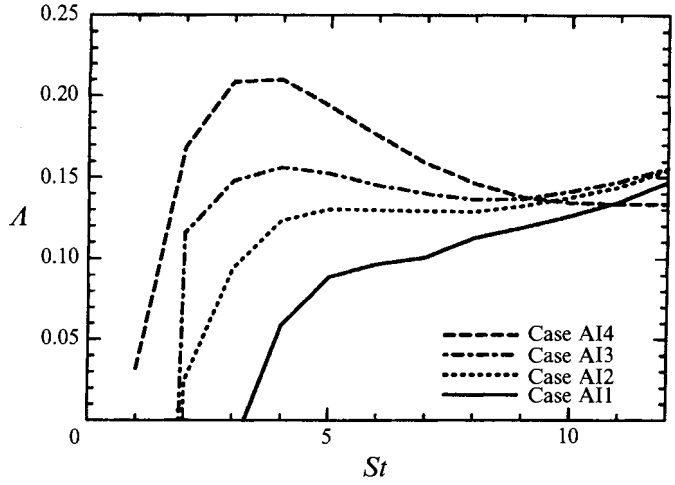

FIGURE 5. Evolution of the turbulent energy growth rate Λ from DNS of incompressible homogeneous shear flow. Cases AI1, AI2, AI3 and AI4 have the same initial data, shear rate S and viscosity ν as cases A1, A2, A3 and A4, respectively. However, cases AI1–AI4 are simulations of the incompressible Navier–Stokes equations, while A1–A4 consider the compressible counterpart.

due to compressibility. Figure 4(*c*) shows the evolution of the correlation coefficient $R(u,v) = \overline{u'v'}/(u_{rms}v_{rms})$. The difference in $R(u,v)$ among cases is not as dramatic as that in the Reynolds stress anisotropies.

The gradient Mach number is changed in series A by changing the shear rate S. A legitimate concern is that increasing S in the *incompressible* case may lead to decreased turbulence growth rates and the observed reduction of Λ in series A may not be a 'compressibility effect' after all. In order to address this concern, four cases AI1, AI2, AI3 and AI4 were performed where the incompressible Navier–Stokes equations were simulated. The initial data and parameters were identical for AI1 and A1, for AI2 and A2, for AI3 and A3, and for AI4 and A4 except that the incompressible Navier–Stokes equations were numerically solved in cases AI1–AI4 in contrast to the simulation of the compressible Navier–Stokes equations in cases A1–A4. Since the speed of sound $c = \infty$ in the incompressible case, the gradient Mach number and turbulent Mach number are both zero in cases AI1–AI4. The initial values of SK/ϵ in cases AI1, AI2, AI3 and AI4 are 1.8, 3.6, 5.4, and 10.8 respectively. Figure 5 shows the evolution of turbulent energy growth rate Λ in the incompressible simulations. The simulations had to be terminated by $St = 12$ so as to preserve good resolution of the small scales. The difference between the long-time growth rates among cases AI1–AI3 is small and, furthermore, the higher shear case AI3 seems to have a slightly larger value of Λ at the end of the simulation than the low shear case AI1, contrary to the dramatic reduction with increased shear observed in the compressible simulations. However, the highest shear case AI4 has a slightly reduced growth rate, probably because the initial value of $SK/\epsilon = 10.8$ is large enough to cause some rapid distortion effects in the turbulence evolution. Overall, it is clear that the reduced turbulence growth rate seen in series A of the simulations is indeed a compressibility effect.

4.2. *DNS results on the turbulence growth in series B*

The effect of increasing M_{t0}, keeping M_{g0} constant, on the turbulence growth rate is investigated in series B of the simulations. According to the DNS, Λ evolves to asymptotic values that show a systematic decrease with increasing M_{t0}. Figure 6 shows

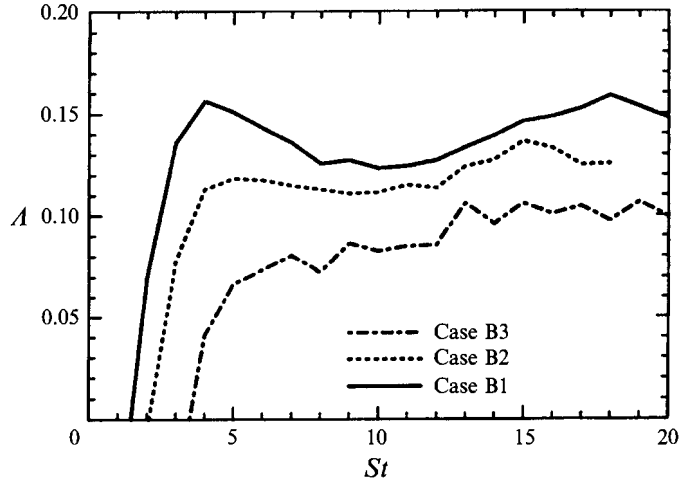

FIGURE 6. Evolution of the turbulent energy growth rate Λ for series B of the homogeneous shear DNS.

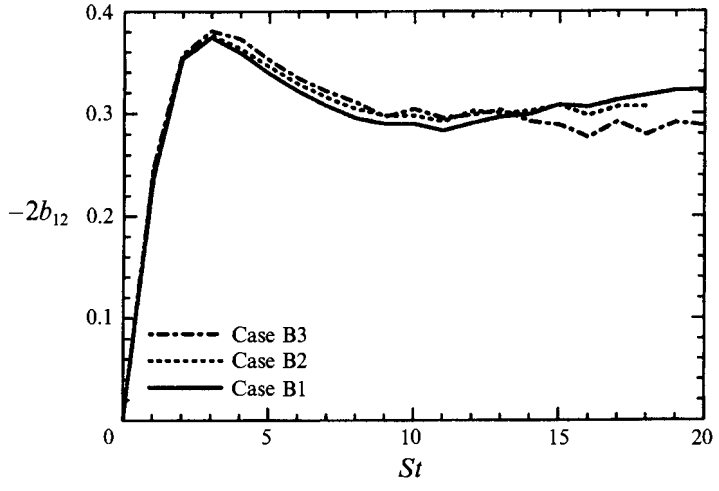

FIGURE 7. Evolution of the non-dimensional production $\mathscr{P}/SK = -2b_{12}$ in series B of the homogeneous shear DNS.

that the high M_{t0} case B3 has an asymptotic value $\Lambda_\infty \approx 0.11$ which is smaller than the corresponding value $\Lambda_\infty \simeq 0.15$ in the low M_{t0} case B1. Although significant, the reduction is not as large as in series A where the high M_{g0} case A4 has a growth rate $\Lambda_\infty = 0.03$ which is only a third of that in case A1.

Equation (19) is again used to distinguish between the contribution of production, dissipation and explicit dilatational terms to the observed 'compressibility effect' of reduced turbulence growth rate. Figures 7 and 8(*a*) show the evolution of normalized production $-2b_{12}$, and the relative dissipation $\epsilon_s/\mathscr{P}$, respectively. Comparison of cases B1 and B3 in figures 7 and 8(*a*) show that case B3 has a lower production level and higher dissipation level relative to case B1. This difference leads to the lower value of Λ for case B3 relative to case B1 in figure 6. Figure 8(*b*) shows the evolution of the pressure–dilatation and compressible dissipation; the cases with higher M_{t0} have larger

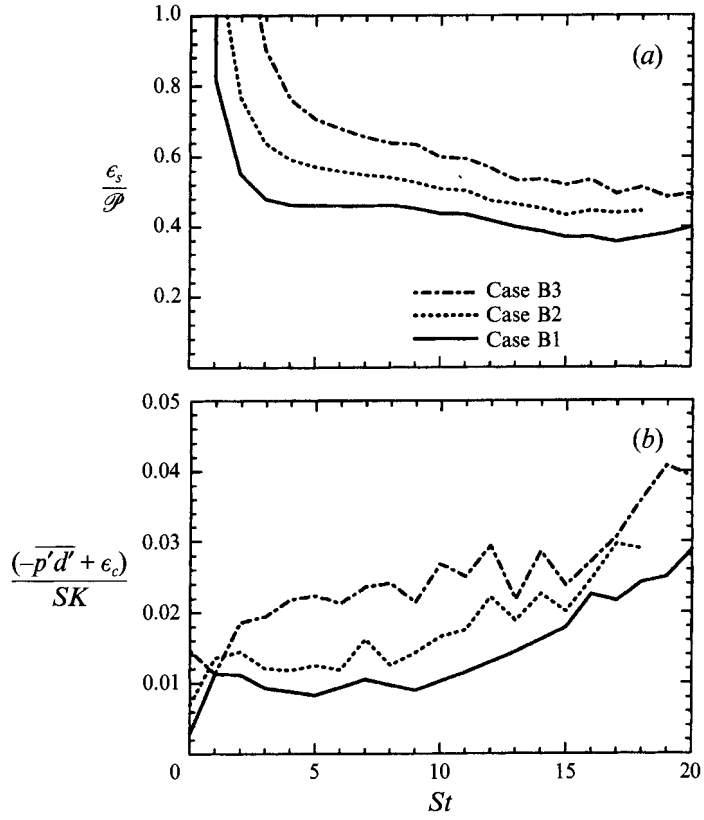

FIGURE 8. Evolution of (*a*) the relative dissipation $\epsilon_s/\mathscr{P}$ and (*b*) the dilatational terms in the K-equation for series B of the homogeneous shear flow DNS.

dilatational contributions to the normalized growth rate. However, the difference in the dilatational terms among the various cases in figure 8(*b*) is small.

Thus, the compressibility effect of decreased growth rate of turbulent kinetic energy in series B is due to both a reduced level of production and an increase in the relative contribution of the turbulent dissipation rate. This is in contrast with series A of the simulations where the reduced level of production is solely responsible for the reduced growth rate of turbulent kinetic energy.

4.3. *Consolidated results from series* A *and* B

The growth rate A_∞ of the turbulent kinetic energy ranges from a high of 0.15 in case B1 to a low of 0.03 in case A4. Thus, compressibility has a strong 'stabilizing' effect on the turbulence growth. This occurs in spite of rather small values of the dilatational component of velocity; the compressible fraction of turbulent kinetic energy χ_K is always less than 10% at the end of each simulation. However, the influence of compressibility on the pressure field is much more significant, as shown below. A method to quantify compressibility effects on the pressure is provided by the pressure decomposition (Erlebacher *et al.* 1990; Sarkar 1992) which splits the pressure field at a given time into $p' = p^{I'} + p^{C'}$, where the incompressible pressure $p^{I'}$ satisfies

$$\nabla^2 p^{I'} = -2\bar{U}_{i,j}(\bar{\rho}u_j^{I'})_{,i} - 2\bar{U}_{i,i}(\bar{\rho}u_j^{I'})_{,j} - (\bar{\rho}u_i^{I'}u_j^{I'})_{,ij} - 2\bar{U}_{i,ij}(\bar{\rho}u_j^{I'}) \tag{23}$$

while the remainder $p^{C'}$ is the compressible pressure. Thus, (23), which is a Poisson

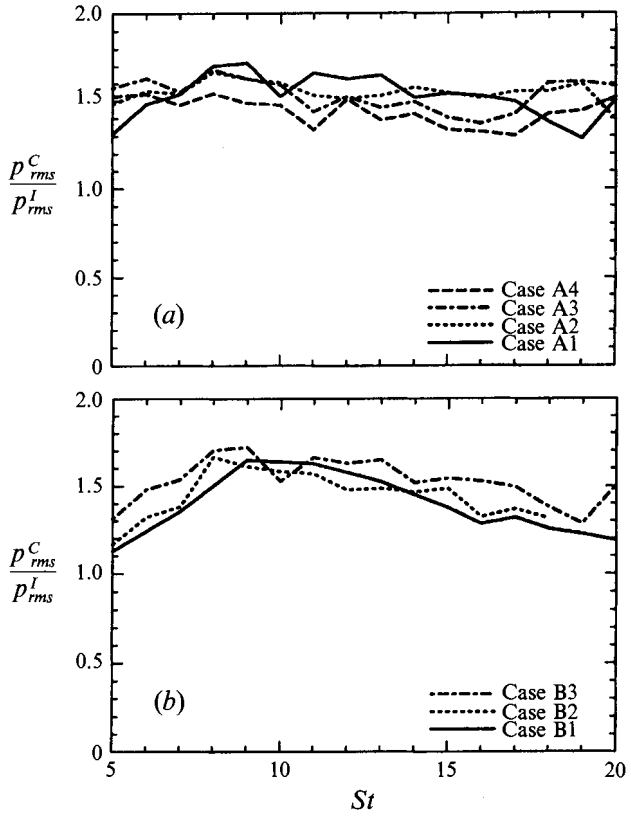

FIGURE 9. Effect of (*a*) initial gradient Mach number and (*b*) initial turbulent Mach number on the evolution of compressible pressure in homogeneous shear flow.

equation for $p^{I'}$, has right-hand side terms that involve $\bar{\rho}$ and is free of ρ' terms. Although the pressure decomposition is not unique, unlike the corresponding Helmholtz decomposition for the velocity, it is a useful method to quantify deviations of the pressure field from the baseline incompressible behaviour. In the simulations, since p' is available from the compressible Navier–Stokes solution and $p^{I'}$ is evaluated from (23), we obtain $p^{C'}$ as the difference $p'-p^{I'}$. Figures 9(*a*) and 9(*b*) show the evolution of the ratio p^C_{rms}/p^I_{rms} in series A and B, respectively. It is clear that the 'compressible pressure' fluctuation $p^{C'}$ unlike the dilatational velocity fluctuation, is comparable to and actually larger than the incompressible counterpart. Figures 10(*a*) and 10(*b*) show the evolution of the correlation coefficient $R(p_C, p_I) = \overline{p^{C'}p^{I'}}/(p^C_{rms}p^I_{rms})$. A systematic increase in the magnitude of $R(p_C, p_I)$ from the low-M_{g0} case A1 to the high-M_{g0} case A4 is evident in figure 10(*a*). Also, the magnitude of $R(p_C, p_I)$ is generally larger in series A relative to series B. It appears from figures 9 and 10 that compressibility has a significant quantitative effect on the pressure field. The consequent effect on the pressure–strain correlation in the Reynolds stress transport equations could lead to the reduction in the magnitude of the anisotropy of the Reynolds shear stress b_{12}, and the observed increase (not discussed in detail here) in the magnitude of the normal stress anisotropy. Thus, pressure–strain models that are used for incompressible flows may not be applicable to high-speed shear flows.

The gradient Mach number and turbulent Mach number evolve in time because of the temporal evolution in the transverse lengthscale l and the kinetic energy K,

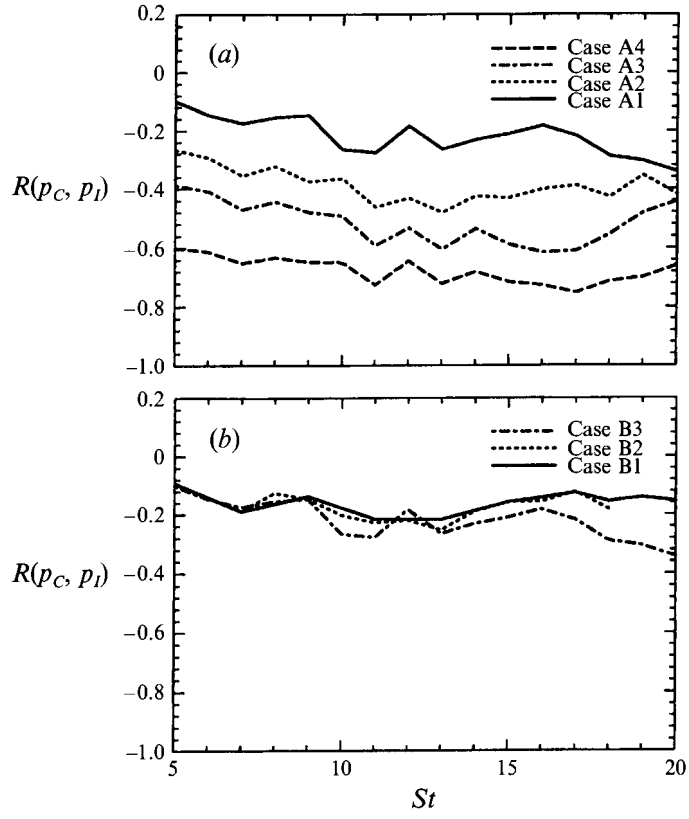

FIGURE 10. Effect of (*a*) initial gradient Mach number and (*b*) initial turbulent Mach number on the evolution of pressure correlation coefficient in homogeneous shear flow.

respectively. A plausible locality hypothesis for the influence of Mach number is that, after the initial transient and for sufficiently high Reynolds number, the value of either M_g or M_t or both at a given time determines the value of turbulence growth rate A at that time. From figures 1 and 6, it appears that A eventually becomes approximately constant in time. Therefore, if either M_g or M_t shows a similar tendency to become invariant with time in the DNS, the locality hypothesis about the influence of Mach number would be supported. Figures 11(*a*) and 11(*b*) show the evolution of M_t in series A and B, respectively. Of the seven cases, only case A4 shows a possible tendency of M_t to become constant. M_t exhibits a monotonic increase with time in all other cases. Thus, the DNS data on the long-time behaviour of M_t do not support the hypothesis that the instantaneous value of M_t determines the turbulence growth rate. Figures 12(*a*) and 12(*b*) show the evolution of M_g in series A and B, respectively. According to figure 12(*a*), the $M_g(St)$ curve tends to flatten with increasing St in cases A1–A3. Figure 12(*b*) shows that, after an initial increase in the series B simulations, M_g decreases slightly for large time. Since the large eddies are constrained by the finite dimensions of the computational box, l stops increasing eventually and $M_g = Sl/\bar{c}$ stops increasing. The DNS data of figure 12 shows a tendency for M_g to become eventually constant and provide some support for the hypothesis that the turbulence growth rate depends on the instantaneous value of the gradient Mach number M_g. Assuming that such a hypothesis is meaningful, we plot A_∞ normalized by the incompressible value of 0.15 in our DNS against the terminal value of M_g in figure 13.

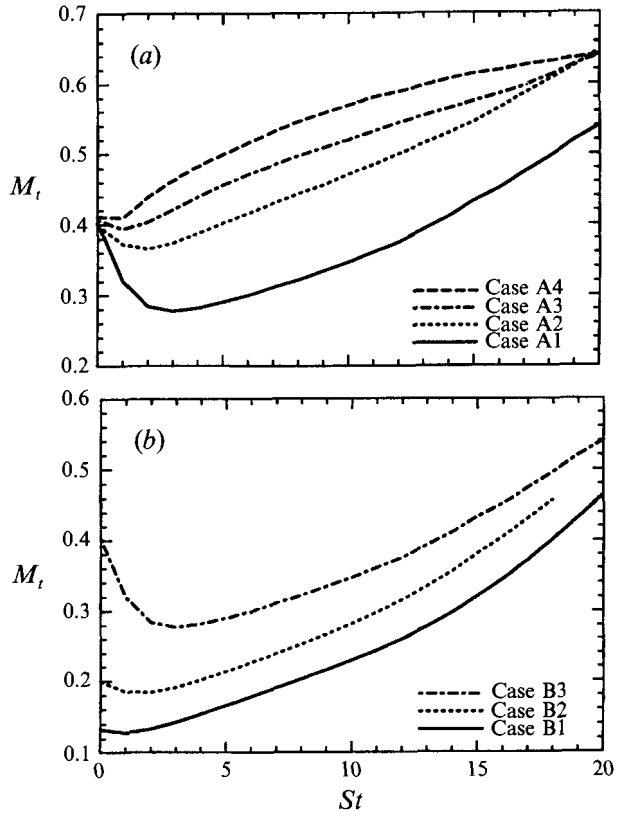

FIGURE 11. The evolution of turbulent Mach number in (*a*) series A and (*b*) series B of the DNS of homogeneous shear flow.

According to figure 13, there is a large reduction of the normalized turbulence growth rate in homogeneous shear flow when M_g increases. The similarity of the curve in figure 13 with the variation (Kline *et al.* 1982; Papamoschou & Roshko 1988) of thickness growth rate $\mathrm{d}\delta/\mathrm{d}x$ with convective Mach number M_c is evident. This similarity between the compressibility effect on the growth rate of turbulent kinetic energy in homogeneous shear flow and the compressibility effect on the thickness growth rate of the turbulent mixing layer is not surprising in view of (17) that relates the thickness growth rate $\mathrm{d}\delta/\mathrm{d}x$ to the kinetic energy growth rate Λ.

5. Implications of the DNS results for compressible shear flows

The reduced growth rate of turbulent kinetic energy (and all its components) observed in the DNS of compressible homogeneous shear flow is analogous to the reduction in turbulence intensities (Elliott & Samimy 1990; Barre, Quine & Dussauge 1994) and thickness growth rate in the high-speed mixing layer. Inspection of (17) shows that the streamwise growth rate $\mathrm{d}\delta/\mathrm{d}x$ of the mixing layer is proportional to Λ_∞/C_2, where Λ_∞ is the asymptotic growth rate of turbulent energy in the corresponding homogeneous shear flow problem, and C_2 is defined by (15). Thus, the mixing layer growth rate $\mathrm{d}\delta/\mathrm{d}x$ will decrease with increasing Mach number if either of the following factors occurs: (i) The asymptotic growth rate Λ_∞ of K in the

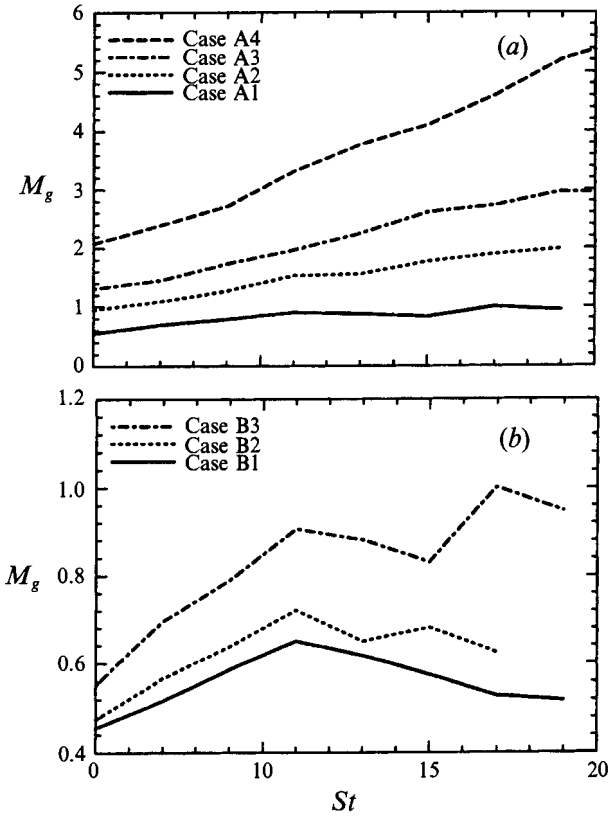

FIGURE 12. The evolution of gradient Mach number in (*a*) series A and (*b*) series B of the DNS of homogeneous shear flow.

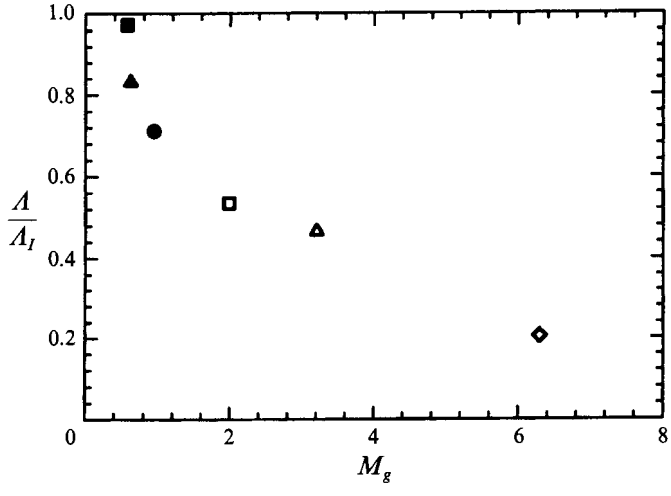

FIGURE 13. The dependence of the asymptotic growth rate of turbulent kinetic energy on the final values of gradient Mach number in the DNS. Open symbols refer to series A while filled symbols refer to series B.

corresponding homogeneous shear problem reduces. (ii) The coefficient c_2 increases, that is the convection velocity U_c becomes a relatively larger fraction of (U_1+U_2).

According to our DNS, the first of the above conditions is met. Experimental or simulation data are required to investigate whether the second factor occurs. Thus, the decrease of A_∞ with the increase in Mach number that is observed in our DNS is consistent with the experimentally observed reduction in the growth rate of mixing layer thickness. More importantly, the phenomenon of reduced 'efficiency' of turbulence production by shear that occurs in the homogeneous shear flow DNS may be an important contributor to the reduced shear layer growth observed in experiments on the compressible mixing layer. A recent numerical study by Papamoschou & Lele (1993) of the evolution of the disturbance field of a small isolated vortex placed in a hyperbolic-tangent mean flow profile has found that the growth rate of the perturbation energy decreases owing to reduced production at high convective Mach numbers. Although the conditions (such as a small-amplitude disturbance and isolated vortex) considered by Papamoschou & Lele (1993) are very different from those in the present DNS of homogeneous shear flow, it is interesting to note that both studies find that compressibility reduces the Reynolds shear stress.

The effect of gradient Mach number M_g appropriately defined using the mean compression rate $D = |\nabla \cdot \bar{U}|$ instead of the shear rate S has been investigated by Jacquin *et al.* (1993) for the shock/turbulence interaction problem and by Cambon *et al.* (1993) for the case of homogeneous compression in the rapid distortion theory (RDT) limit, that is for $DK/\epsilon \gg 1$. Both investigations found that the growth of turbulent kinetic energy increases monotonically with the gradient Mach number, in contrast to the finding of the present paper. Of course, the present work differs in two crucial aspects from that of Jacquin *et al.* (1993) and Cambon *et al.* (1993) which may account for the different results. First, shear flow is considered here instead of compressed flow; and second, the mean shear rate is moderate so that nonlinear effects are important in the present work while nonlinear effects are negligible with respect to the large mean strain in the RDT approach used by the other authors.

It is well known (Bradshaw 1977; Lele 1994) that compressibility effects over and above the influence of mean density are much stronger in the mixing layer than the boundary layer. The mean Mach number, either free-stream M_∞ in the boundary layer or convective M_c in the mixing layer, may take the same value, say 2; however, at this value of Mach number, the boundary layer does not show the large reduction in thickness growth rate that the shear layer does. This suggests that there may be another non-dimensional parameter based on the speed of sound which could conceivably distinguish between the boundary layer and the shear layer by taking different values although the mean Mach number is the same in these flows. We now show that the gradient Mach number M_g could be such a parameter by estimating its value in the boundary layer and the mixing layer.

Consider the adiabatic zero-pressure-gradient boundary layer on a flat plate. The gradient Mach number

$$M_g = \frac{(\mathrm{d}\bar{U}/\mathrm{d}y)\,l}{\bar{c}}, \tag{24}$$

in the log-region, which occupies a large portion of the boundary layer, is estimated as follows. The Van Driest scaling for the law of the wall (Bradshaw 1977) in the adiabatic compressible boundary layer,

$$\frac{\mathrm{d}\bar{U}}{\mathrm{d}y} = \frac{(\tau_w/\bar{\rho})^{1/2}}{\kappa y}, \tag{25}$$

where τ_w is the wall shear stress and κ the von Kármán constant, is used for the mean shear rate. Since the active shear-stress-producing motion scales with distance from the wall (Townsend 1980), the approximate relation $l \approx y$ is used for the integral lengthscale. Thus, (24) becomes

$$M_g = \frac{(\tau_w/\bar{\rho})^{1/2}}{\kappa \bar{c}} = \frac{M_\tau}{\kappa}. \tag{26}$$

Here $M_\tau = (\tau_w/\bar{\rho}_w)^{1/2}/\bar{c}_w$ is the friction Mach number based on wall friction and thermodynamic properties at the wall. The relation $M_\tau = M_\infty (C_f/2)^{1/2}$ which links the friction Mach number to the free-stream Mach number is now substituted into (26) to give

$$M_g \approx \frac{M_\infty (C_f/2)^{1/2}}{\kappa}. \tag{27}$$

Thus, the gradient Mach number is a constant given by (27) in the log-region of the high-speed boundary layer.

We now consider the mixing layer. The mean velocity U in the mixing layer between two streams with velocities U_1 and U_2, respectively, is assumed (Schlichting 1979) to behave like an error-function,

$$\frac{U-U_2}{U_1-U_2} = \frac{1+\mathrm{erf}(\eta)}{2}, \tag{28}$$

where $\eta = 2(y-y_c)/\delta(x)$ is the similarity coordinate, y_c is the position of the half-velocity point, $\delta(x)$ is the mixing layer thickness, and $\mathrm{erf}(\eta) = (2/\pi^{1/2}) \int_0^\eta \exp(-u^2)\,\mathrm{d}u$. Let us estimate the value of M_g at $\eta = 0$ where the velocity gradient is maximum. From (28), the velocity gradient at $\eta = 0$ is $2(U_1-U_2)/(\pi^{1/2}\delta)$. The lengthscale l of the turbulence is approximated by $l \approx \delta$ which is consistent with the measurements of Wygnanski & Fielder (1970) in an incompressible mixing layer, and the speed of sound at the centre of the mixing layer is taken to be 0.5 $(c_1 + c_2)$. Then, the expression

$$M_g \approx 2.2 M_c \tag{29}$$

is obtained as an estimate for the gradient Mach number at the centreline.

We now compare the variation of M_g as a function of M_∞ and M_c, respectively, for the mixing layer and the boundary layer. The Van Driest II expression for $C_f(M_\infty)$ which agrees well with experimental data (Bradshaw 1977) is used in (27) to obtain M_g as a function of M_∞ in the boundary layer. The momentum thickness Reynolds number for the boundary layer is chosen to be $Re_\theta = 10^4$. The solid curve in figure 14 displays the variation of M_g at the mixing layer centreline given by (29), while the dashed curve shows the variation of M_g in the log-region of the boundary layer represented by (27). It is clear that the gradient Mach number M_g for the mixing layer becomes much larger than that for the boundary layer when the mean Mach number increases. The smallness of M_g in the boundary layer relative to the shear layer is a crucial difference between the two flows that could account for the much smaller compressibility effect in the boundary layer relative to the shear layer. The turbulence production level is observed to decrease in our DNS when M_g increases. Thus, on the basis of these considerations, the compressibility effect that reduces turbulence production is expected to be far smaller in a boundary layer relative to the mixing layer even if the mean flow Mach numbers have the same value in the two cases. This expectation is borne out by experimental results for the two flows.

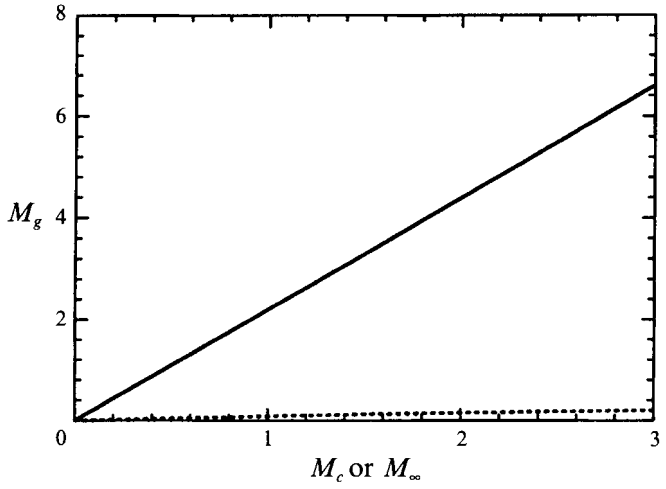

FIGURE 14. The variation of gradient Mach number M_g in the mixing layer (——) and the boundary layer (·····). The abscissa is the convective Mach number M_c for the mixing layer curve and free-stream Mach number M_∞ for the boundary layer curve.

6. Conclusions

DNS of a compressible fluid in turbulent homogeneous shear flow is performed for several cases in order to investigate and clarify some aspects of the influence of compressibility on turbulence. The two Mach numbers relevant to homogeneous shear flow – the turbulent Mach number M_t and the gradient Mach number M_g – were prescribed to have different initial values in the simulations. The initial value of M_g is varied keeping the initial value of M_t constant in series A of the simulations, and vice versa in series B. Although the Reynolds number $Re_\lambda \approx 40$ at the end of the simulations is moderate, it is large enough for the flow to be turbulent. A total of six 128^3 simulations are performed. The simulations are used to investigate the influence of compressibility on the normalized growth rate of the turbulent kinetic energy K given by $A = (1/SK)(\mathrm{d}K/\mathrm{d}t)$ where S is the mean shear rate. The behaviour of A is important because it is shown here through an analogy to be proportional to the thickness growth rate of the corresponding inhomogeneous mixing layer. The DNS results show that homogeneous shear flow, which is perhaps the simplest example of a turbulent shear flow, is strongly affected by compressibility. The asymptotic growth rate A_∞ of the turbulent kinetic energy decreases when either the initial gradient Mach number M_{g0} or the initial turbulent Mach number M_{t0} is increased, and furthermore the reduction is substantially larger in the situation where M_{g0} is increased. This 'stabilizing' effect of compressibility is analogous to the reduction in turbulent intensities and thickness growth rate observed in experiments on the high-speed mixing layer. It may be noted that the inhibited growth of turbulence in homogeneous shear flow is not a mean density effect, since the initial mean density is constant between cases and does not change with flow evolution.

The asymptotic growth rate of the turbulent kinetic energy depends on the eventual balance between the turbulent production by shear, the turbulent dissipation, and dilatational terms. A systematic comparison of these terms in the different cases is performed in order to identify probable causes for the reduced growth rate. Such a comparison leads to the conclusion that the reduction in the Reynolds shear stress anisotropy b_{12} and consequent reduction in the turbulence production level is

predominantly responsible for the reduced growth rate of the turbulent kinetic energy. The dilatational terms (pressure dilatation and compressible dissipation) are not negligible in the sense that they are observed to be as large as 20% of the turbulent kinetic energy budget. However, the difference in the values of the growth rate A among different cases is not due to differences in the dilatational terms.

The gradient Mach number M_g appears to be an important parameter in compressible shear flows. The turbulent energy growth rate decreases significantly when the gradient Mach number increases as shown in figure 13. For example, the growth rate is only half of its incompressible value at $M_g = 2$. We have estimated the value of M_g as a function of the convective Mach number M_c in the mixing layer and as a function of the free-stream Mach number M_∞ in the wall boundary layer. The parameter M_g increases significantly more rapidly in the mixing layer than in the boundary layer, when the mean Mach number of the flow (M_c in the mixing layer or M_∞ in the boundary layer) increases. For example, a supersonic shear layer with $M_c = 1$ has $M_g \approx 2.2$, while a supersonic boundary layer with $M_\infty = 2$, $Re_\theta = 10^4$ has $M_g \approx 0.16$. It is well known that explicit compressibility effects over and above the effect of variable mean density are much larger in the supersonic shear layer relative to the supersonic boundary layer. Since the reduction in turbulence production by the mean shear and the consequent 'stabilizing' effect of compressibility in turbulent shear flows appears to be a strong function of the gradient Mach number in our DNS study, a possible reason for the difference between the extent of compressibility effects in the high-speed mixing layer and boundary layer is the large difference in values of the parameter M_g.

Comments by J. Lasheras and P. A. Libby on a preliminary draft of the manuscript are appreciated. This work was supported by NASA grant NAG 1-1516 and originated during a stay at ICASE.

REFERENCES

BARRE, S., QUINE, C. & DUSSAUGE, J. P. 1994 Compressibility effects on the structure of supersonic mixing layers: experimental results. *J. Fluid Mech.* **259**, 47–78.

BLAISDELL, G. A., MANSOUR, N. N. & REYNOLDS, W. C. 1993 Compressibility effects on the growth and structure of homogeneous turbulent shear flow. *J. Fluid Mech.* **256**, 443–485.

BRADSHAW, P. 1977 Compressible turbulent shear layers. *Ann. Rev. Fluid Mech.* **9**, 33–54.

CAMBON, C., COLEMAN, G. N. & MANSOUR, N. N. 1993 RDT and DNS of compressible homogeneous turbulence at finite Mach number. *J. Fluid Mech.* **257**, 641–665.

DURBIN, P. A. & ZEMAN, O. 1992 Rapid distortion theory for homogeneous compressed turbulence with application to modelling. *J. Fluid Mech.* **242**, 349–370.

ELLIOTT, G. S. & SAMIMY, M. 1990 Compressibility effects in free shear layers. *Phys. Fluids* A **2**, 1231–1240.

ERLEBACHER, G., HUSSAINI, M. Y., KREISS, H. O. & SARKAR, S. 1990 The analysis and simulation of compressible turbulence. *Theoret. Comput. Fluid Dyn.* **2**, 73–95.

FEIEREISEN, W. J., SHIRANI, E., FERZIGER, J. H. & REYNOLDS, W. C. 1982 Direct simulation of homogeneous turbulent shear flows on the Illiac IV computer: applications to compressible and incompressible modelling. In *Turbulent Shear Flows 3* (ed. L. J. S. Bradbury *et al.*) pp. 309–319.

JACKSON, T. L. & GROSCH, C. E. 1990 Absolute/convective instabilities and the convective Mach number in a compressible mixing layer. *Phys. Fluids* A **2**, 949–954.

JACQUIN, L., CAMBON, C. & BLIN, E. 1993 Turbulence amplification by a shock wave and rapid distortion theory. *Phys. Fluids* A **5**, 2539–2550.

KLINE, S. J., CANTWELL, B. J. & LILLEY, G. M. 1982 *Proc. 1980–81 AFOSR–HTTM–Stanford Conf. on Complex Turbulent Flows*, vol. 1, Stanford University Press.

LEE, M. J., KIM, J. & MOIN, P. 1990 Structure of turbulence at high shear rate. *J. Fluid Mech.* **216**, 561–583.

LELE, S. K. 1994 Compressibility effects on turbulence. *Ann. Rev. Fluid Mech.* **26**, 211–254.

MORRIS, P. J., GIRIDHARAN, M. G. & LILLEY, G. M. 1990 On the turbulent mixing of compressible free shear layers. *Proc. R. Soc. Lond.* A **431**, 219–243.

PAPAMOSCHOU, D. & LELE, S. K. 1993 Vortex-induced disturbance field in a compressible shear layer. *Phys. Fluids* A **5**, 1412–1419.

PAPAMOSCHOU, D. & ROSHKO, A. 1988 The compressible turbulent shear layer: an experimental study. *J. Fluid Mech.* **197**, 453–477.

RAGAB, S. A. & WU, J. L. 1989 Linear instabilities in two-dimensional compressible mixing layers. *Phys. Fluids* A **1**, 957–966.

ROGERS, M. M., MOIN, P. & REYNOLDS, W. C. 1987 The structure of the vorticity field in homogeneous turbulent flows. *J. Fluid Mech.* **176**, 33–66.

SANDHAM, N. D. & REYNOLDS, W. C. 1991 Three-dimensional simulations of large eddies in the compressible mixing layer. *J. Fluid Mech.* **224**, 133–158.

SARKAR, S. 1992 The pressure-dilatation correlation in compressible flows. *Phys. Fluids* A **4**, 2674–2682.

SARKAR, S., ERLEBACHER, G. & HUSSAINI, M. Y. 1991*a* Direct simulation of compressible turbulence in a shear flow. *Theor. Comput. Fluid Dyn.* **2**, 291–305.

SARKAR, S., ERLEBACHER, G., HUSSAINI, M. Y. & KREISS, H. O. 1991*b* The analysis and modelling of dilatational terms in compressible turbulence. *J. Fluid Mech.* **227**, 473–493.

SCHLICHTING, H. 1979 *Boundary-Layer Theory*, 7th edn. McGraw-Hill.

SPEZIALE, C. G. 1991 Analytical methods for the development of Reynolds-stress closures in turbulence. *Ann. Rev. Fluid Mech.* **23**, 107–157.

TAVOULARIS, S. & KARNIK, U. 1989 Further experiments on the evolution of turbulent stresses and scales in uniformly sheared turbulence. *J. Fluid Mech.* **204**, 457–478.

TOWNSEND, A. A. 1980 *The Structure of Turbulent Shear Flow*, 2nd edn. Cambridge University Press.

WYGNANSKI, I. & FIEDLER, H. E. 1970 The two-dimensional mixing region. *J. Fluid Mech.* **41**, 327–361.

ZEMAN, O. 1990 Dilatation dissipation – the concept and application in modelling compressible mixing layers. *Phys. Fluids* A **2**, 178–188.